Vol. No.5, Issue No. 10, October 2016 www.ijarse.com



# UNSTEADY MIXED CONVECTION FLOW OVER EXPONENTIALLY PERMEABLE STRETCHING SURFACE THROUGH POROUS MEDIUM IN PRESENCE OF CHEMICAL REACTION, SORET AND DUFOUR EFFECTS

## Nafisa A. Kumbarwadi

Department of Mathematics, KarnatakUniversity, Pawate Nagar, Dharwad, Karnataka, (India)

#### **ABSTRACT**

This article deals with the unsteady double diffusive mixed convection flow over exponentially permeable vertical stretching surface through Darcy-Forchheimer porous medium in presence of chemical reaction, Dufour and Soret (cross diffusion) effects. The unsteadiness in the flow, temperature and species concentration fields is due to time dependent free stream velocity and stretching sheet velocity. The non-dimensional equations are obtained from governing equations by employing the implicit finite difference method in combination with Quasi-linearization technique. Numerical computations are presented graphically to show the chemical reaction, Soret, Dufour and permeability effects on temperature, velocity and species concentration profiles. The results for heat transfer, the skin friction and mass transfer coefficient are also presented. The present results are excellent as compared with previously published work.

Keywords: Exponentially Stretching Surface, Unsteady Mixed Convection, Non-Similar Solution, Darcy-Forchheimer Porous Medium, Chemical Reaction, Dufour And Soret Effects.

#### I. INTRODUCTION

The fluid flow through porous medium has attracted the attention of many researchers/scientists due to their wide applications in technology and industry, also in natural circumstances, such as in the field of agricultural engineering to study the underground water resources, seepage of water in river beds, in petroleum technology to study the movement of natural gas, oil and water through oil reservoirs, in chemical engineering for filtration and purification process (Hayat *et al.* [1]), the dispersion of chemical contaminants, in chemical catalytic reactors, in thermal insulation, in storage and disposal of chemical and nuclear waste material, pollutant dispersion in aquifers, packed bed reactors, geothermal extraction, cooling of electronic components, food processing, casting and welding of manufacturing processes(Patil *et al.* [2]), heat exchangers, soil pollution, fibrous insulation etc. The effect of surface melting on steady, mixed convection, boundary layer flow over a vertical flat surface embedded in a fluid-saturated porous medium examined by Merkin *et al.* [3]. Recently, Swain et al. [4] studied the flow over exponentially stretching sheet through porous medium with heat

Vol. No.5, Issue No. 10, October 2016

#### www.ijarse.com



source/sink. The Darcy law, which states that the volume averaged velocity is proportional to the pressure gradient, is only suitable for low velocity viscous fluid flows and fluid with small porosity (Hong *et al.* [5]). But the Darcy law is not applicable in many practical situations, like porous medium bounded by impermeable wall, higher fluid flow rates and non-uniform porosity distribution near wall region. Therefore, it is essential to incorporate the non-Darcian terms in the study of the convective transport in a porous medium (K. Das [6]). The inertia effect is expected to be more important at high flow rate hence velocity squared term is added to momentum equation, which is known as the Forchheimer drag parameter. Kumari *et. al* [7] investigated non-similar solution of non-Darcy mixed convection flow in saturated porous medium.

Flow and heat transfer from an exponentially stretching surface has wide applications in science and technology, for example in case of annealing and thinning of copper wires the final product depends on the rate of heat transfer at the continuous stretching surface with exponential variations of stretching surface velocity and temperature distribution. Raju *et al.* [8] investigated heat and mass transfer in magnetohydrodynamics Casson depends on the rate of heat transfer at the continuous stretching surface with exponential variations of stretching surface velocity and temperature distribution. Heat and mass transfer over exponentially stretching continuous surface was investigated by Magyari and Keller [9]. Unsteady mixed convection flows do not necessarily permit similarity solutions in many practical situations. The unsteadiness and non-similarity occur due to the time dependent free stream velocity as well as wall stretching velocity. Due to the mathematical complexity in obtaining non-similar solutions for such flow problems, many investigators have restricted their investigation\ analysis either to an unsteady similar flows or steady non-similar flows (Patil *et al.* [10]). Patil *et al.* [11] have investigated unsteady two-dimensional mixed convection flow along a vertical power-law stretching sheet in a parallel free stream with a power-law wall temperature distribution.

The energy flux caused by concentration gradient is termed as Dufour effect and the mass flux due to temperature gradient is known as Soret effect. In most of the studies these effects are neglected because of their smaller orders of magnitude described by Fick's and Fourier laws. Recently, the developments in this area show that these effects are identical when density differences exist in the fluid flow. Generally, Soret and Dufour effects are taken as second order phenomenon. The Dufour and Soret (cross diffusion) effects have many practical applications such as the ground water migration, the solidification of binary alloys, and in the areas of geosciences, and chemical engineering. The Soret effect, for instance has been utilized for isotope separation and in mixture between gases with very light molecular weight and of medium molecular weight (M. B. K Moorthy et al. [12]) and also in natural hydrocarbon reservoirs. The effect of Dufour was in considerable magnitude such that it cannot be neglected. Shrinivacharya and RamReddy[13] investigated mixed convection flow over exponentially stretching surface in presence of Non-Darcy porous medium, soret and dufour effects. Heat and mass transfer with chemical reaction has numerous practical applications in industry and technology, such as in drying and cooling processes etc. Suction/injection (blowing) of a fluid over a stretching surface can influence the flow field. In general suction tends to enhance the skin friction, heat transfer, and mass transfer coefficients, whereas injection acts in opposite manner. The processes of suction/injection has many practical applications in science and engineering, such as distribution of temperature and moisture over agricultural fields and groves of fruit trees, in the design of thrust bearing and radial diffuser, and thermal oil recovery etc. Suction is applied to chemical processes to remove reactants. Injection or blowing is use to cool surface, prevent

Vol. No.5, Issue No. 10, October 2016

## www.ijarse.com

IJARSE ISSN (O) 2319 - 8354 ISSN (P) 2319 - 8346

corrosion or scaling and reduce the drag, polymer fiber coating, and coating of wires etc (Patil *et al.* [14]). Effect of heat source or sink on unsteady flow and heat transfer with suction or blowing studied by Cheng *et. al* [15].

The aim of the present paper is to explore the effects of unsteady mixed convection flows over exponentially permeable stretching sheet through porous medium with Chemical reaction, Soret and Dufour effects. This work has not been reported in the literature so far to the authors best of knowledge. Non-similar transformations are used to transform the governing boundary layer equations to a set of non-dimensional equations and then numerically solved by Quasi-linearization technique [16] in combination with the implicit finite difference scheme. We found that the numerical results are excellent as compared with previous published data.

#### II. ANALYSIS

Consider an unsteady double diffusive mixed convection boundary layer flow bounded by a semi-infinite vertical permeable exponentially stretching sheet embedded in a Darcy-Forchheimer porous medium. Also, we consider the Dufour and Soret effects. The x-axis is taken along the plate in the vertically upward direction and the y-axis is taken normal to it. Figure 1 shows the schematic representation of the physical model and coordinate system. The buoyancy force arises due to the concentration and temperature variations, and body force arises because of density variations except these effects all thermo-physical properties of the fluid are assumed to be constant. The Boussinesq approximation is invoked for the fluid properties to relate density changes, and to couple the temperature and species concentration fields to the flow field (Schlichting and Gersten[17]). Under these assumptions, the equations of conservation of mass, momentum, temperature and species concentration governing flow over exponentially stretching sheet are given by [2]

$$\frac{\partial u}{\partial x} + \frac{\partial v}{\partial y} = 0,\tag{1}$$

$$\frac{\partial u}{\partial t} + u \frac{\partial u}{\partial x} + v \frac{\partial u}{\partial y} = \frac{\partial U_e}{\partial t} + U_e \frac{dU_e}{dx} + v \frac{\partial^2 u}{\partial y^2} + g \left[ \beta \left( T - T_{\infty} \right) + \beta^* \left( C - C_{\infty} \right) \right] - \frac{\varepsilon v}{K} \left( u - U_e \right) - \frac{S \varepsilon^2}{K^{\frac{1}{2}}} \left( u^2 - U_e^2 \right), \tag{2}$$

$$\frac{\partial T}{\partial t} + u \frac{\partial T}{\partial x} + v \frac{\partial T}{\partial y} = \alpha \frac{\partial^2 T}{\partial y^2} + \frac{D_m k_T}{C_s C_p} \frac{\partial^2 C}{\partial y^2},$$
(3)

$$\frac{\partial C}{\partial t} + u \frac{\partial C}{\partial x} + v \frac{\partial C}{\partial y} = D \frac{\partial^2 C}{\partial y^2} + \frac{D_m k_T}{T_m} \frac{\partial^2 T}{\partial y^2} - R(x) (C - C_{\infty}), \tag{4}$$

The physical boundary conditions are given by

Vol. No.5, Issue No. 10, October 2016

## www.ijarse.com

IJARSE ISSN (O) 2319 - 8354 ISSN (P) 2319 - 8346

$$y = 0: u = U_W(x, t), v = v_w, T = T_W = T_\infty + (T_{W0} - T_\infty) \exp\left(\frac{2x}{L}\right),$$

$$C = C_W = C_\infty + (C_{W0} - C_\infty) \exp\left(\frac{2x}{L}\right),$$

$$y \to \infty: u \to U_x(x, t), \qquad T \to T_\infty, \qquad C \to C_\infty. \tag{5}$$

The wall stretching sheet velocity  $U_{w}(x)$  and free stream velocity  $U_{e}(x)$  are respectively defined by

$$U_{\scriptscriptstyle W}(x,t) = U_{\scriptscriptstyle 0}\phi\big(\tau\big)\exp\bigg(\frac{x}{L}\bigg), U_{\scriptscriptstyle e}(x,t) = U_{\scriptscriptstyle \infty}\phi\big(\tau\big)\exp\bigg(\frac{x}{L}\bigg), \text{ where } U_{\scriptscriptstyle 0} \text{ is the reference velocity, } U_{\scriptscriptstyle \infty} \text{ is }$$

the free stream velocity and L is the characteristic length.

Applying the following

$$\xi = \frac{x}{L}, \eta = \left(\frac{U_0}{vx}\right)^{1/2} \exp\left(\frac{x}{2L}\right) y, \tau = \frac{U_0^2 \exp\left(\frac{x}{L}\right)}{v} t,$$

$$\psi(x, y, t) = (vU_0 x)^{1/2} \exp\left(\frac{x}{2L}\right) \phi(\tau) f(\xi, \eta, \tau),$$

$$T - T_{\infty} = (T_w - T_{\infty}) G(\xi, \eta, \tau), \quad (T_w - T_{\infty}) = (T_{w0} - T_{\infty}) \exp\left(\frac{2x}{L}\right),$$

$$transformations:$$

$$C - C_{\infty} = (C_w - C_{\infty}) H(\xi, \eta, \tau), \quad (C_w - C_{\infty}) = (C_{w0} - C_{\infty}) \exp\left(\frac{2x}{L}\right),$$

$$u = \frac{\partial \psi}{\partial y}, \quad v = -\frac{\partial \psi}{\partial x}, \quad u = U_0 \phi(\tau) \exp\left(\frac{x}{L}\right) F,$$

$$v = -\frac{1}{2} \left(\frac{vU_0}{x}\right)^{1/2} \phi(\tau) \exp\left(\frac{x}{2L}\right) \left\{ (1 + \xi) f + 2\xi f_{\xi} + \eta (\xi - 1) F + \tau \xi (f_{\tau} + \phi_{\tau} \phi^{-1} f) \right\},$$
(6)

to Eqs. (1) - (4), we find that Eq. (1) is trivially satisfied, and Eqs. (2) - (4) reduce to

Vol. No.5, Issue No. 10, October 2016

www.ijarse.com



$$F_{\eta\eta} + \phi(\tau) [(1+\xi)\frac{f}{2} + \xi \tau (f_{\tau} + \phi_{\tau} \phi^{-1}(\tau)f)] F_{\eta} - \phi \xi F^{2} - \phi(\tau) \{ \xi \tau (F_{\tau} + \phi_{\tau} \phi^{-1}(\tau)F) \} F^{-1} + \phi \xi F^{2} - \phi(\tau) \{ \xi \tau (F_{\tau} + \phi_{\tau} \phi^{-1}(\tau)F) \} F^{-1} + \phi \xi F^{2} - \phi(\tau) \{ \xi \tau (F_{\tau} + \phi_{\tau} \phi^{-1}(\tau)F) \} F^{-1} + \phi \xi F^{2} - \phi(\tau) \{ \xi \tau (F_{\tau} + \phi_{\tau} \phi^{-1}(\tau)F) \} F^{-1} + \phi \xi F^{2} - \phi(\tau) \{ \xi \tau (F_{\tau} + \phi_{\tau} \phi^{-1}(\tau)F) \} F^{-1} + \phi \xi F^{2} - \phi(\tau) \{ \xi \tau (F_{\tau} + \phi_{\tau} \phi^{-1}(\tau)F) \} F^{-1} + \phi \xi F^{2} - \phi(\tau) \{ \xi \tau (F_{\tau} + \phi_{\tau} \phi^{-1}(\tau)F) \} F^{-1} + \phi \xi F^{2} - \phi(\tau) \{ \xi \tau (F_{\tau} + \phi_{\tau} \phi^{-1}(\tau)F) \} F^{-1} + \phi \xi F^{2} - \phi(\tau) \{ \xi \tau (F_{\tau} + \phi_{\tau} \phi^{-1}(\tau)F) \} F^{-1} + \phi \xi F^{2} - \phi(\tau) \{ \xi \tau (F_{\tau} + \phi_{\tau} \phi^{-1}(\tau)F) \} F^{-1} + \phi \xi F^{2} - \phi(\tau) \{ \xi \tau (F_{\tau} + \phi_{\tau} \phi^{-1}(\tau)F) \} F^{-1} + \phi \xi F^{2} - \phi(\tau) \{ \xi \tau (F_{\tau} + \phi_{\tau} \phi^{-1}(\tau)F) \} F^{-1} + \phi \xi F^{2} - \phi(\tau) \{ \xi \tau (F_{\tau} + \phi_{\tau} \phi^{-1}(\tau)F) \} F^{-1} + \phi \xi F^{2} - \phi(\tau) \{ \xi \tau (F_{\tau} + \phi_{\tau} \phi^{-1}(\tau)F) \} F^{-1} + \phi \xi F^{2} - \phi(\tau) \} F^{-1} + \phi \xi F^{-1} + \phi \xi F^{2} - \phi(\tau) \} F^{-1} + \phi \xi F^{-1} + \phi$$

$$-\xi\operatorname{Re}\phi^{-1}(\tau)\phi_{\tau}F - \operatorname{Re}\xi F_{\tau} + \xi\operatorname{Re}\phi^{-1}(\tau)\phi_{\tau}\beta + \beta^{2}\xi(\phi(\tau) + \tau\phi_{\tau}) + Ri\xi\phi^{-1}(\tau)(g + Nh)$$

$$-\frac{\xi e^{-\xi}}{Da\operatorname{Re}} (F-\beta) - \xi \phi(\tau) \Gamma (F^2 - \beta^2) = \xi \phi(\tau) \{F F_{\xi} - f_{\xi} F_{\eta}\}, \tag{7}$$

$$G_{\eta\eta} + \Pr\phi(\tau) \left\{ (1+\xi) \frac{f}{2} + \tau \xi (f_{\tau} + \phi^{-1}(\tau)\phi_{\tau} f) \right\} G_{\eta} - 2\phi(\tau) \Pr\xi F G - \xi \Pr(\operatorname{Re} + \phi(\tau)\tau F) G_{\tau}$$

$$+\operatorname{Pr}D_{f}H_{\eta\eta}=\operatorname{Pr}\xi\phi(\tau)\big\{FG_{\xi}-f_{\xi}G_{\eta}\big\},\tag{8}$$

$$H_{\eta\eta} + Sc\phi(\tau) \left\{ (1+\xi)\frac{f}{2} + \xi \tau (f_{\tau} + \phi^{-1}(\tau)\phi_{\tau}f) \right\} H_{\eta} - 2Sc\xi\phi(\tau)FH - Sc\Delta\xi\beta H$$

$$-\xi Sc(\operatorname{Re} + \phi(\tau)\tau F)H_{\tau} + ScSrG_{\eta\eta} = Sc\xi\phi(\tau)\left\{FH_{\xi} - f_{\xi}H_{\eta}\right\}. \tag{9}$$

The non-dimensional boundary conditions (5) become

$$\eta = 0 : F = 1, G = 1, H = 1,$$

$$\eta \to \infty: F \to \beta, G \to 0, H \to 0, \tag{10}$$

Here  $f(\xi, \eta) = \int_{0}^{\eta} F d\eta + f_{W}$  and  $f_{W}$  can be obtained from transformations as,

$$v = -\frac{1}{2} \left( \frac{vU_0}{x} \right)^{1/2} \phi(\tau) \exp\left( \frac{x}{2L} \right) \left\{ (1+\xi)f + 2\xi f_{\xi} + \eta(\xi - 1)F + \tau \xi (f_{\tau} + \phi_{\tau}\phi^{-1}f) \right\}$$

In view of boundary condition (5) and  $v_w = v_0 \exp\left(\frac{x}{2L}\right)$ , we get

$$i.e., \left\{ (1+\xi)f_W + 2\xi (f_{\xi})_W + \tau \xi ((f_{\tau})_w + \phi_{\tau W}\phi^{-1}f_w) \right\} = A \frac{\xi^{1/2}}{\phi(\tau)}$$

where  $A = -2v_0 \left(\frac{L}{vU_0}\right)^{1/2} = \text{constant}$ , is the surface mass transfer parameter with A > 0 for the suction,

A < 0 for the injection or blowing and A = 0 for an impermeable surface.

Vol. No.5, Issue No. 10, October 2016

## www.ijarse.com



The momentum Eq. (7), the energy Eq. (8) and the species concentration Eq. (9) are coupled with each other. Further, the Richardson number Ri, which characterizes the mixed convection effects, N representing the ratio between the thermal and the solutal buoyancy forces,  $\beta$  is the velocity ratio parameter,  $\Delta$  is chemical effect, Da is Darcy number,  $\Gamma$  is Forchheimer drag coefficient, Df is the Dufour number and Sr is the Soret number and they are defined, respectively, as

$$Ri = \frac{Gr}{\text{Re}^2}, \ N = \frac{Gr^*}{Gr}, \ \beta = \frac{U_{\infty}}{U_0}, \ \Delta = \frac{R_0L}{U_{\infty}}, \ Da = \frac{K}{\varepsilon L^2}, \ \Gamma = \frac{S\varepsilon^2}{K^{1/2}}, \ Df = \frac{D_m k_T}{v C_s C_p} \left(\frac{C_w - C_{\infty}}{T_w - T_{\infty}}\right)$$

and 
$$Sr = \frac{D_m k_T}{v T_m} \left( \frac{T_w - T_\infty}{C_w - C_\infty} \right)$$
, (11)

where  $Gr = g \ \beta (T_{w0} - T_{\infty}) L^3 / v^2$  is the Grashof number referring to the wall temperature,  $Gr^* = g \ \beta^* (C_{w0} - C_{\infty}) L^3 / v^2$  is the Grashof number referring to the wall species concentration and  $\operatorname{Re} = U_0 L / v$  is the Reynolds number. The flow is steady at  $\tau = \mathbf{O}$  and becomes unsteady  $\tau > \mathbf{O}$  due to exponentially stretching wall velocity varies with time, and this wall velocity given by  $U_w(x) = U_0 \phi(\tau) \exp\left(\frac{x}{L}\right)$  and free stream velocity  $U_e(x) = U_\infty \phi(\tau) \exp\left(\frac{x}{L}\right)$ , where  $\phi(\tau) = 1 + \alpha \tau^2$ .

Hence, the initial conditions (i.e. conditions at  $\tau=0$ ) are given by the steady state equations obtained from (7) - (9) by substituting  $d\phi/d\tau = F_{\tau} = G_{\tau} = H_{\tau} = 0$ ,  $\phi(\tau)=1$  when  $\tau=0$  [11].

The physical quantities of practical interest are given by the Nusselt number Nu, the skin friction coefficient  $C_f$ , and the Sherwood number Sh, which represent the shear stress, the mass transfer rate and the heat transfer rate at the surface, respectively. These coefficients are defined, respectively, as

$$C_f = \mu \frac{2(\partial u/\partial y)_{y=0}}{\rho U_w^2} = 2 \operatorname{Re}^{-1/2} \xi^{-1/2} \exp(\xi)^{-1/2} \phi^{-1} F_{\eta}(\xi, 0),$$

i.e., 
$$\left(\text{Re }\xi\exp(\xi)\right)^{1/2}C_f = 2\phi^{-1}F_\eta(\xi,0).$$
 (12)

$$Nu = -x \frac{\left(\partial T/\partial y\right)_{y=0}}{\left(T_{w} - T_{\infty}\right)} = -\left(\operatorname{Re} \xi \exp(\xi)\right)^{1/2} G_{\eta}(\xi, 0),$$

i. e., 
$$\left( \text{Re } \xi \exp(\xi) \right)^{-1/2} Nu = -G_{\eta}(\xi, 0).$$
 (13)

$$Sh = -x \frac{\left(\partial C/\partial y\right)_{y=0}}{\left(C_{w} - C_{\infty}\right)} = -\left(\operatorname{Re} \xi \exp(\xi)\right)^{1/2} H_{\eta}(\xi, 0),$$

i.e., 
$$\left(\operatorname{Re}\xi\exp(\xi)\right)^{-1/2}Sh = -H_{\eta}(\xi,0).$$
 (14)

Vol. No.5, Issue No. 10, October 2016

## www.ijarse.com

## III. METHOD OF SOLUTION

IJARSE
ISSN (0) 2319 - 8354
ISSN (P) 2319 - 8346

The numerical method used for this investigation is the implicit finite difference method. A central difference formula is applied across the boundary layer direction  $i.\ e.,\ \eta$  - direction and backward difference formula in streamwise  $\xi$  and time  $\tau$  directions. After we apply Quasi-linearization technique[16] to solve the non-dimensional equation. The application of this technique is quadratic rate of convergence. Using this technique the non-linear coupled partial differential equations are transformed to linear partial differential equations as following

$$F_{\eta\eta}^{i+1} + A_1^i F_{\eta}^{i+1} + A_2^i F^{i+1} + A_3^i F_{\xi}^{i+1} + A_4^i F_{\tau}^{i+1} + A_5^i G^{i+1} + A_6^i H^{i+1} = A_7^i,$$
 (15)

$$G_{\eta\eta}^{i+1} + B_1^i G_{\eta}^{i+1} + B_2^i G^{i+1} + B_3^i G_{\xi}^{i+1} + B_4^i G_{\tau}^{i+1} + B_5^i F_{\eta}^{i+1} + B_6^i H_{\eta\eta}^{i+1} = B_7^i,$$
 (16)

$$H_{nn}^{i+1} + C_1^i H_n^{i+1} + C_2^i H^{i+1} + C_3^i H_{\varepsilon}^{i+1} + C_4^i H_{\tau}^{i+1} + C_5^i F^{i+1} + C_6^i G_{nn}^{iA+1} = C_7^i.$$
 (17)

The coefficient functions with iterative index i are known and the functions with iterative index (i+1) are to be determined. The corresponding boundary conditions are given by

$$F^{i+1}(\xi,0) = 1, \quad G^{i+1}(\xi,0) = 1, \quad H^{i+1}(\xi,0) = 1 \quad \text{at} \quad \eta = 0,$$

$$F^{i+1}(\xi,\eta) = \beta, \quad G^{i+1}(\xi,\eta) = 0, \quad H^{i+1}(\xi,\eta) = 0 \quad \text{at} \quad \eta = \eta_{c}.$$
(18)

The final equations were then formed to a system of linear algebraic equations with a block tri-diagonal matrix, which is then solved by Varga's algorithm [18]. We have chosen step sizes of  $\Delta \eta$ ,  $\Delta \xi$  and  $\Delta \tau$  as 0.01, 0.01 and 0.01, respectively, which ensure the convergence of the numerical solution to the exact solution. A convergence criterion based on the relative difference between the current and previous iteration values is employed. The numerical solution is assumed to have converged and the iteration process is terminated when the difference reaches less than  $10^{-5}$ , *i. e.*,

$$\operatorname{Max}\left\{ \left| \left( F_{\eta} \right)_{w}^{i+1} - \left( F_{\eta} \right)_{w}^{i} \right|, \left| \left( G_{\eta} \right)_{w}^{i+1} - \left( G_{\eta} \right)_{w}^{i} \right|, \left| \left( H_{\eta} \right)_{w}^{i+1} - \left( H_{\eta} \right)_{w}^{i} \right| \right\} < 10^{-5}. \tag{19}$$

The present numerical results are compared with the results previously reported by Magyari and keller[9] and Srinivasacharya and Ramreddy[13] to validate the accuracy and convergence. The results are found to be in excellent agreement as given in **Table 1**.

In support of non-similar solutions the effects of all the physical parameters involved in the problem, some of the numerical results pertaining to skin friction parameter  $(Re)^{1/2} C_f$ , heat transfer

Parameter  $(Re)^{-1/2} Nu$  and mass transfer parameter  $(Re)^{-1/2} Sh$  are tabulated in **Table 2**.

#### IV. RESULTS AND DISCUSSION

The system of dimensionless non-linear coupled partial differential equations (7) - (9) under the boundary conditions (10) have been solved numerically by using Quasi-linearization technique [23] with implicit finite difference scheme. The numerical computations have been carried out for various values of Ri ( $-1 \le Ri \le 3$ ),  $\beta$  ( $0.5 \le \beta \le 1.5$ ),

Vol. No.5, Issue No. 10, October 2016

## www.ijarse.com

IJARSE ISSN (O) 2319 - 8354 ISSN (P) 2319 - 8346

 $Df(0.1 \le Df \le 1.5)$ ,  $Pr(0.7 \le Pr \le 7.0)$ ,  $Sc(0.66 \le Sc \le 2.57)$ ,  $Sr(0.1 \le Sr \le 1.5)$ ,  $\Gamma(0.0 \le \Gamma \le 2.0)$ ,

 $\alpha \ (-0.2 \le \alpha \le 0.2), \ \tau \ (0 \le \tau \le 1), \ N(-1 \le N \le 3), \ Da(1.0 \le Da \le 1000000).$  The edge of the

boundary layer  $\eta_{\infty}$  has been taken between 4.0 and 10.0 depending on the values of the governing parameters.

The numerical results have been obtained for both accelerating  $[\phi(\tau) = 1 + \alpha \tau^2; \alpha > 0, 0 \le \tau \le 1]$  and decelerating  $[\phi(\tau) = 1 + \alpha \tau^2; \alpha < 0, 0 \le \tau \le 1]$  free stream velocities of the fluid. It may be noted that the range of parameter values is used for air and water at different temperatures. For example, Pr = 0.7 for air, Pr = 7.0 for water at  $20^{\circ}C$  and the value of Pr reduces for water at higher temperature.

The effects of Reynolds (Re) number and time ( $\tau$ ) on velocity profile ( $F(\xi, \eta, \tau)$ ) for accelerating flow  $\phi(\tau) = 1 + \alpha \tau^2$ ,  $\alpha = 1$  when

 $\beta$ =0.5, N=1.0,  $\Delta$ =0.5,  $\Gamma$ =1.0, Re=2.0, Ri=1.0, Pr=0.7, Df=0.5, Sr=0.5,

Sc=0.94, Da=1.0 and A=1.0, is shown in Fig. 2. It is observed that the velocity profile is decreasing with increase of Re and  $\tau$ . Physically, the Reynolds number measures the relative velocity of the flow. Thus the velocity increases with increasing values of Reynolds number, which reduces the magnitude of velocity profile. For instance,  $\alpha=1$ , Re=2,  $\beta=0.5$ , Df=0.5, Sr=0.5,  $\Gamma=0.5$ , N=1, A=1, Da=1,  $\Delta=0.5$ , the velocity profile decreases by 13% and 6% with increasing values of Re from 10 to 50 along with increasing values of time  $\tau$  from 0 to 1.

Figure 3 shows the effects of Forchheimer's drag coefficient ( $\Gamma$ ) and time  $\tau$  on velocity profile  $F(\xi,\eta,\tau)$  for accelerating flow

 $\phi(\tau) = 1 + \alpha \tau^2$ ,  $\alpha = 1.0$  when Re = 1,  $\beta = 0.5$ , Ri = 1, Pr = 0.7, Df = 0.5, Sr = 0.5, N = 1.0,

 $\xi = 1, Sc = 0.94, A = 1, Da = 1$ . It shows that the magnitude of the velocity profile decreases with increase of Forchheimer's drag coefficient  $(\Gamma)$ . Also, the momentum boundary layer thickness reduces as time  $\tau$  increases from 0 to 1.

The effects of N and  $\tau$  on  $F(\xi,\eta,\tau)$  for  $\alpha=2.0$ , Pr=0.7, Sc=0.94, Sr=0.5, Df=0.5,  $\xi=1.0$ , Ri=1,  $\beta=0.5$ ,  $\Gamma=0.5$ , Da=1 and A=1 are plotted in Fig. 4. The velocity overshoot increase with increase of buoyancy forces parameter N. It is clear that assisting buoyancy ratio parameter N>0, acts like favourable pressure gradient, which accelerates the flow and overshoot occurs in velocity profile. The unsteadiness parameter  $\tau$  shows the significant effect on velocity profile, the velocity profile decreases with increase of time  $\tau$  from 0 to 1. Thus, the momentum boundary thickness reduces with increase of  $\tau$  from 0 to 1. In particular, for

example,  $\alpha = 2$ , Re = 1,  $\beta = 0.5$ , Ri = 1, Pr = 0.7,

 $Df = 0.5, Sr = 0.5, \Gamma = 0.5, \Delta = 0.5, A = 1, Da = 1$ , the velocity profile decreases by 10% and 27% as increases of N from -1 to 1 and increase of  $\tau$  from  $\tau = 0$  to  $\tau = 1$ . Fig. 5 illustrate the effects of N and Da on

Vol. No.5, Issue No. 10, October 2016

## www.ijarse.com

IJARSE ISSN (O) 2319 - 8354 ISSN (P) 2319 - 8346

 $\left(\operatorname{Re}\right)^{1/2}C_f$  for both the accelerating  $\phi(\tau)=1+\alpha\tau^2$ ,  $\alpha=-0.5$  and decelerating flow  $\phi(\tau)=1+\alpha\tau^2$ ,  $\alpha=-0.5$  when Ri=1,  $\xi=1.0$ , Sc=0.94,

Re = 2,  $\Gamma$  = 0.5, Pr = 0.7, Sr = 0.5, Df = 0.5, Da = 1,  $\Delta$  = 0.5, A = 1. The skin friction parameter  $\left(\text{Re}\right)^{1/2}C_f$  increases with increase of N from -1 to 1. The reason is that higher values of N, implies the assisting pressure gradient and fluid moves faster with high velocity. The skin friction coefficient increases for accelerating flow and decreases for decelerating flow. In particular, when Ri = 1,  $\xi$  = 1.0, Sc = 0.94, Re = 2,  $\Gamma$  = 0.5, Pr = 0.7, Sr = 0.5, Df = 0.5, Da = 1,  $\Delta$  = 0.5, A = 1,  $\left(\text{Re}\right)^{1/2}C_f$  increases approximately by 53% and 46% with the increase in  $\alpha$  from -0.5 to 0.5.

Figure 6 shows the effects of Dufour number (Df) and time  $\tau$  on temperature profile  $G(\xi,\eta,\tau)$  for  $\alpha=2$ , Ri=1,  $\xi=1$ , Sc=0.94, N=1, Re=2 and  $\Gamma=1$ ,  $\beta=0.5$ , Sr=0.5, Da=1,  $\Delta=0.5$ , A=1. The effect of dufour term on temperature profile is highly significant because the dufour term appears only in temperature equation, which enhances the thermal boundary layer thickness. Further, the unsteadiness decreases the thermal boundary layer thickness. For example, when  $\alpha=2$ , Ri=1,  $\xi=1$ , Sc=0.94, N=1, Re=2 and  $\Gamma=1$ ,  $\beta=0.5$ , Sr=0.5, Da=1,  $\Delta=0.5$ , A=1, temperature profile decreases 85% and 39% with increasing values of time  $\tau$  from  $\tau=0$  to  $\tau=1$ , with Df=0.1 and Df=1.0 respectively.

The variations of Dufour number (Df) and surface mass transfer (A) on  $(Re)^{-1/2} Nu$  heat transfer coefficient is plotted in Fig. 7 for

 $Ri=1, \xi=1.0, \text{Sc}=0.94, N=1.0, \text{Re}=2, \text{Pr}=0.7, \Gamma=0.5, \beta=0.5, Sr=0.5 \text{ and } A=1. \text{ The heat transfer coefficient } \left(\text{Re}\right)^{-1/2} Nu$  increases with the increase of A from A = -1 to 1. Further,  $\left(\text{Re}\right)^{-1/2} Nu$  decreases with increase of Dufour number from 0.1 to 1. Physically, the dufour number is ratio of concentration difference to the temperature. The heat transfer increases with suction (A>0) and decreases with injection (A<0). In particular, for instance for decelerating flow  $\phi(\tau)=1+\alpha\tau^2, \alpha=-0.5$  when  $Ri=1, \xi=1, N=1, N=1$ 

Re = 2,  $\Gamma$  = 0.5,  $\beta$  = 1.5, Df = 0.5, Da = 1 the  $\left(\text{Re}\right)^{-1/2} Nu$  decreases 42% and 36% with the increase of Df from 0.1 to 1.0, and with the increase of A for -1 to 1, respectively.

Figure 8 illustrates the effects Schmidt number (Sc) and time  $\tau$  on concentration profile for accelerating flow  $\phi(\tau) = 1 + \alpha \tau^2$ ,  $\alpha = 1$  with N = 1, Ri = 1.0,  $\xi = 1$ , Pr = 0.7,  $\Gamma = 1$ ,  $\beta = 0.5$ , Df = 0.5, Da = 1. It is evident that the increase of time decreases the concentration profile. Further, increase in the Schmidt number, the concentration profile decreases. The reason is the Schmidt number means decrease of diffusivity that results in decrease of concentration boundary layer thickness. For instance, for accelerating flow  $\phi(\tau) = 1 + \alpha \tau^2$ ,  $\alpha = 1$  with N = 1, Ri = 1.0,  $\xi = 1$ , Pr = 0.7,  $\Gamma = 1$ ,  $\beta = 0.5$ , Df = 0.5, Da = 1 the

Vol. No.5, Issue No. 10, October 2016

#### www.ijarse.com

JARSE ISSN (O) 2319 - 8354 ISSN (P) 2319 - 8346

concentration profile decreases 26% and 43% with the increase of Sc from 0.22 to 0.94, and with the increase of  $\tau$  from 0 to 1, respectively.

Figure 9 displays the effects of chemical reaction parameter  $\Delta$  and Soret number Sr on  $(Re)^{-1/2}Sh$  (Sherwood number or mass transfer coefficient) for accelerating flow  $\phi(\tau) = 1 + \alpha \tau^2$ ,  $\alpha > 0$  and decelerating flow  $\phi(\tau) = 1 + \alpha \tau^2$ ,  $\alpha < 0$  when  $Ri = 1, \xi = 1.0, Df = 0.5$ , Sc = 0.94, N = 1.0, Pr = 0.7, Re = 2,  $\Gamma = 0.5$ ,  $\beta = 1.5$ , Da = 1 and A = 1. It is clearly observed that  $(Re)^{-1/2}Sh$  decreases with increase of Soret number. Physically, the Soret number is ratio of temperature gradient to concentration. Further, Chemical reaction parameter shows the significant role in mass transfer, while the Sherwood number increases with increase of chemical reaction parameter. The physical reason is that the species generation  $(\Delta > 0)$  effect reduces the concentration boundary layer thickness. Thus, the mass transfer coefficient increases with increase of chemical reaction parameter. For example, when Ri = 1,  $\xi = 1.0$ , Df = 0.5, Sc = 0.94, N = 1.0, Pr = 0.7, Re = 2,  $\Gamma = 0.5$ ,  $\beta = 1.5$ , Da = 1 and A = 1,  $\alpha = -0.5$ ,  $(Re)^{-1/2}Sh$  increases 21% and 31% with increase of Soret number Sr from 0.1 to 1 and with increase of chemical reaction parameter  $\Delta$  from -0.5 to 1.0, respectively.

#### V. CONCLUSION

A numerical study is carried out for the unsteady mixed convection flow over permeable exponentially stretching surface through Darcy-Forchheimerporous medium in presence of cross diffusion (Dufour and Soret) and chemical reaction effects. The resulting system of dimensionless coupled nonlinear partial differential equation was solved by using an implicit finite difference scheme in combination with Quasi-linearization technique. From this numerical investigation the following conclusions are drawn

- The velocity profile increases with increasing values of buoyancy forces parameter and it decreases with increasing values of Forchheimer drag coefficient.
- The temperature profile increases with increasing values of Dufour number and concentration profile decreases with increasing values of Schmidt number.
- The skin friction coefficient increases with increase in buoyancy forces parameter. Further, Suction increases the skin friction, mass transfer and heat transfer coefficient.
- The mass transfer coefficient increases, with increase of chemical reaction parameter and decreases of Soret number.

#### VI. ACKNOWLEDGEMENTS

Nafisa. A. Kumbarwadi expresses her sincere thanks to the UGC New Dehli-110 002 for award of Maulan Azad National Fellowship.

**Table 1.** Values of  $[-g_{\eta}(0)]$  for varius values of Prandtl number Pr with  $\alpha = 0$ , Df = 0, and N = 0,  $Da \to \infty$ ,  $\Delta = 0$ , Sr = Sc = 0, Ri = 0.

Vol. No.5, Issue No. 10, October 2016

## www.ijarse.com

JJARSE ISSN (O) 2319 - 8354 ISSN (P) 2319 - 8346

Pr	0.5	1.0	3.0	5.0	8.0	10.0
Magyari and	-0.59434	-0.95478	-1.86908	-2.50014	-3.24213	-3.66038
Keller[9]						
Srinivasacharya	-0.59438	-0.95478	-1.86908	-2.50015	-3.24218	-3.66043
and Ramreddy[13]						
Present work	-0.59437	-0.95480	-1.86908	-2.50017	-3.24222	-3.66045

**Table. 2:** Values of  $\left(\operatorname{Re}\right)^{1/2}C_f$ ,  $\left(\operatorname{Re}\right)^{-1/2}Nu$ ,  $\left(\operatorname{Re}\right)^{-1/2}Sh$  for different values of Prandtl number Pr with  $\alpha=0.2, \xi=1, \operatorname{Re}=1$ .

Pr	Ri	β	N	Γ	Da	Df	Δ	Sr	Sc	A	τ	$(\mathrm{Re})^{1/2} C_f$	$(Re)^{-1/2} N\iota$	$(Re)^{-1/2} Sh$
0.7	1	1	0.5	0.5	1	0.5	0.5	0.5	0.94	1	1	0.50820	2.51605	3.50285
0.7	1	1	0.5	0.5	1	0.5	0.5	0.5	0.94	1	1.5	0.42483	2.97715	4.03283
0.7	1	1	0.5	0.5	1	0.5	0.5	0.5	0.94	1	2	0.35182	3.53164	4.67637
0.7	1	1.5	0.5	0.5	1	0.5	0.5	0.5	0.94	1	1	3.84100	2.77257	3.84957
0.7	1	1.5	0.5	0.5	1	0.5	0.5	0.5	0.94	1	1.5	6.31817	3.30948	4.45110
0.7	1	1.5	0.5	0.5	1	0.5	0.5	0.5	0.94	1	2	10.48815	3.94448	5.17337
7.0	1	1.0	0.5	0.5	1	0.3	0.5	0.5	0.22	1	1	0.33463	16.87637	0.02493
7.0	1	1.0	0.5	0.5	1	0.3	0.5	0.5	0.22	1	1.5	0.28285	18.60003	0.16304
7.0	1	1.0	0.5	0.5	1	0.3	0.5	0.5	0.22	1	2	0.23723	20.65983	0.33283
7.0	1	1	0.5	0.5	1	0.3	-0.5	0.5	0.22	1	1	0.33920	16.95180	-0.13585
7.0	1	1	0.5	0.5	1	0.3	-0.5	0.5	0.22	1	1.5	0.28600	18.66376	0.02549
7.0	1	1	0.5	0.5	1	0.3	-0.5	0.5	0.22	1	2	0.23921	20.71311	0.21670
7.0	1	1	0.5	0.5	$\infty$	0.3	-0.5	0.5	0.22	1	1	0.34838	16.95277	-0.13510
7.0	1	1	0.5	0.5	$\infty$	0.3	-0.5	0.5	0.22	1	1.5	0.29185	18.66424	0.02574
7.0	1	1	0.5	0.5	$\infty$	0.3	-0.5	0.5	0.22	1	2	0.24297	20.71335	0.21705
0.7	1	1	0.5	0.5	$\infty$	0.5	0.5	0.5	0.94	-1	1	0.48028	1.73493	2.21510
0.7	1	1	0.5	0.5	$\infty$	0.5	0.5	0.5	0.94	-1	1.5	0.41272	2.15812	2.69368
0.7	1	1	0.5	0.5	$\infty$	0.5	0.5	0.5	0.94	-1	2	0.34853	2.68387	3.29531

## Nomenclature

C Species concentration (kg m<sup>-3</sup>)

 $C_f$  Local skin-friction coefficient

## Vol. No.5, Issue No. 10, October 2016

## www.ijarse.com

IJARSE ISSN (0) 2319 - 8354 ISSN (P) 2319 - 8346

- $C_p$  Specific heat at constant pressure (J  $\mathrm{K}^{\text{-1}}\mathrm{kg}^{\text{-1}}$ )
- $C_s$  The concentration susceptibility
- $C_{\rm\scriptscriptstyle w}$  Concentration at the wall (kg m<sup>-3</sup>)
- $C_{w0}$  Reference concentration
- $C_{\scriptscriptstyle \infty}$  Ambient species concentration
- D Mass diffusivity
- Df Dufour number
- Da Darcy number
- f Dimensionless stream function
- R chemical reaction rate
- F Dimensionless velocity
- g Acceleration due to gravity (ms<sup>-2</sup>)
- G Dimensionless temperature
- $Gr, Gr^*$  Grashof numbers due to temperature and species concentration, respectively
- H Dimensionless species concentration
- L characteristic length (m)
- N Ratio of buoyancy forces
- Nu Nusselt number
- Pr Prandtl number  $(\nu/\alpha)$
- Re Reynolds number
- Ri Richardson number
- S Empirical constant in the second-order resistant term
- Sc Schmidt number  $(v/D_m)$
- *Sr* Soret number
- t Time
- T Temperature (K)
- $T_m$  The mean fluid temperature (K)
- $T_{w}$  Temperature at the wall (K)
- $T_{w0}$  Reference temperature
- $T_{\infty}$  Ambient temperature (K)
- $\mathcal{U}$  Velocity component in the  $\mathcal{X}$  direction (m s<sup>-1</sup>)

Vol. No.5, Issue No. 10, October 2016

#### www.ijarse.com

V Velocity component in the Y direction (m s<sup>-1</sup>)

x, y Cartesian coordinates (m)

## **Greek symbols**

- $\alpha$  Thermal diffusivity (m<sup>2</sup> s<sup>-1</sup>)
- $\beta, \beta^*$  Volumetric coefficients of the thermal and concentration expansions, respectively (K<sup>-1</sup>)
- $\xi, \eta, \tau$  Transformed variables
- $\mu$  Dynamic viscosity (kg m<sup>-1</sup> s<sup>-1</sup>)
- V Kinematic viscosity (m<sup>2</sup> s<sup>-1</sup>)
- $\phi(\tau)$  Unsteady function of  $\tau$
- $\rho$  Density (kg m<sup>-3</sup>)
- Ψ Stream function
- Γ Forchheimer's drag parameter

## **Subscripts**

- w condition at the wall
- e free stream condition
- $\xi, \eta, \tau$  Denote the partial derivatives with respect to these variables, respectively.

#### **REFERENCES**

- [1] T. Hayat, Z. Abbas and S. Asgar., Effects of Hall current and heat transfer on rotating flow of a second grade fluid through a porous medium, Comm. Nonlinear. Sci. Numer. Simulat, 13(2008)2177-2192.
- [2] P. M. Patil, A. J. Chamkha., Heat and mass transfer from mixed convection flow of polar fluid along a plate in porous medium with chemical reaction, Int. J. Num. Meth. Heat and Fluid Flow,23(2013)899-926.
- [3] J. H. Merkin, I. Pop, S. Ahmad., Note on the melting effect on mixed convection boundary layer flow over a vertical flat surface embedded in a porous medium, Int. J. Heat Mass Transfer, 84(2015)786-790.
- [4] I. Swain, S. R. Mishra, H. B. Pattanayak., Flow over exponentially stretching sheet through porous medium with heat source/sink, Hindawai. J. Engg(2015).
- [5] J. T. Hong, Y. Yamada, C. L. Tein., Effects of non-Darcian and non-uniform porosity on vertical-plate natural convection in porous media, Trans. ASME J. Heat Transfer, 109(1987) 356.
- [6] K. Das, Convective slip flow of rarefied fluids over a permeable wedge plate embedded in a Darcy-Forcheimer porous medium, Eur. Phys. J. Plus 129(2014)50.
- [7] M. Kumari, I. Pop, G. Nath., Non-similar boundary layer for non-Darcy mixed convection flow about a horizontal surface in a saturated porous medium", Int. J. Engng Sci, 28(1990)253-263.

ISSN (P) 2319 - 8346

Vol. No.5, Issue No. 10, October 2016

#### www.ijarse.com

- IJARSE ISSN (0) 2319 - 8354 ISSN (P) 2319 - 8346
- [8] C. S. K. Raju, N. Sandeep, V. Sugunamma, M. Jayachandra, J. V. Raman Reddy., Heat and mass transfer in magnetohydrodynamic Casson fluid over an exponentially permeable stretching surface, Int. J. Engg. Sci and Tech,19(2016)45-52.
- [9] Magyari. E, Keller., Heat and mass transfer in the boundary layer on an exponentially stretching continuous surface, J. Phys. D. Appl. Phys, 32(1999)577-585.
- [10] P. M. Patil, S. Roy, E. Momoniat., Thermal diffusion and diffusion-thermo effects on mixed convection from an exponentially impermeable stretching surface, Int. J. Heat Mass Transfer, 100(2016)482-489.
- [11] P.M. Patil, S. Roy and I. Pop., Unsteady mixed convection flow over a vertical stretching sheet in a parallel free stream with variable temperature, Int. J. Heat Mass Transfer 53(2010) 4741 4748.
- [12] M. B. K. Moorthy, K. Senthilvadivu., Soret and Dufour Effects on natural convection flow past a vertical surface in a porous medium with variable viscosity, J. Appl. Mathematics, (2012) 1-15.
- [13] D. Srinivasacharya, C. RamReddy., Cross diffusion effects on mixed convection from an exponentially stretching surface in Non-Darcy porous medium, Heat Transfer-Asian Research, 42(2013)111-124.
- [14] P.M. Patil, S. Roy and I. Pop., chemical reaction effects on unsteady mixed convection boundary layer flow past a permeable slender vertical cylinder due to a nonlinearly stretching velocity, Chem. Eng. Comm, 200(2013)398-417.
- [15] W. T. Cheng, C. N. Huang, Unsteady flow and heat transfer on an accelerating surface with blowing or suction in the absence and presence of a heat source or sink, Chem. Engng Sci, 59(2004)771-780.
- [16] K. Inouye, A. Tate., Finite difference version Quasi-linearization applied to boundary layer equations, AIAA J, 12 (1976) 558- 560.
- [17] H. Schlichting, K. Gersten., Boundary Layer Theory, Springer, New York (2000).
- [18] R. S. Varga., Matrix Iterative Analysis, Prentice Hall (2000).



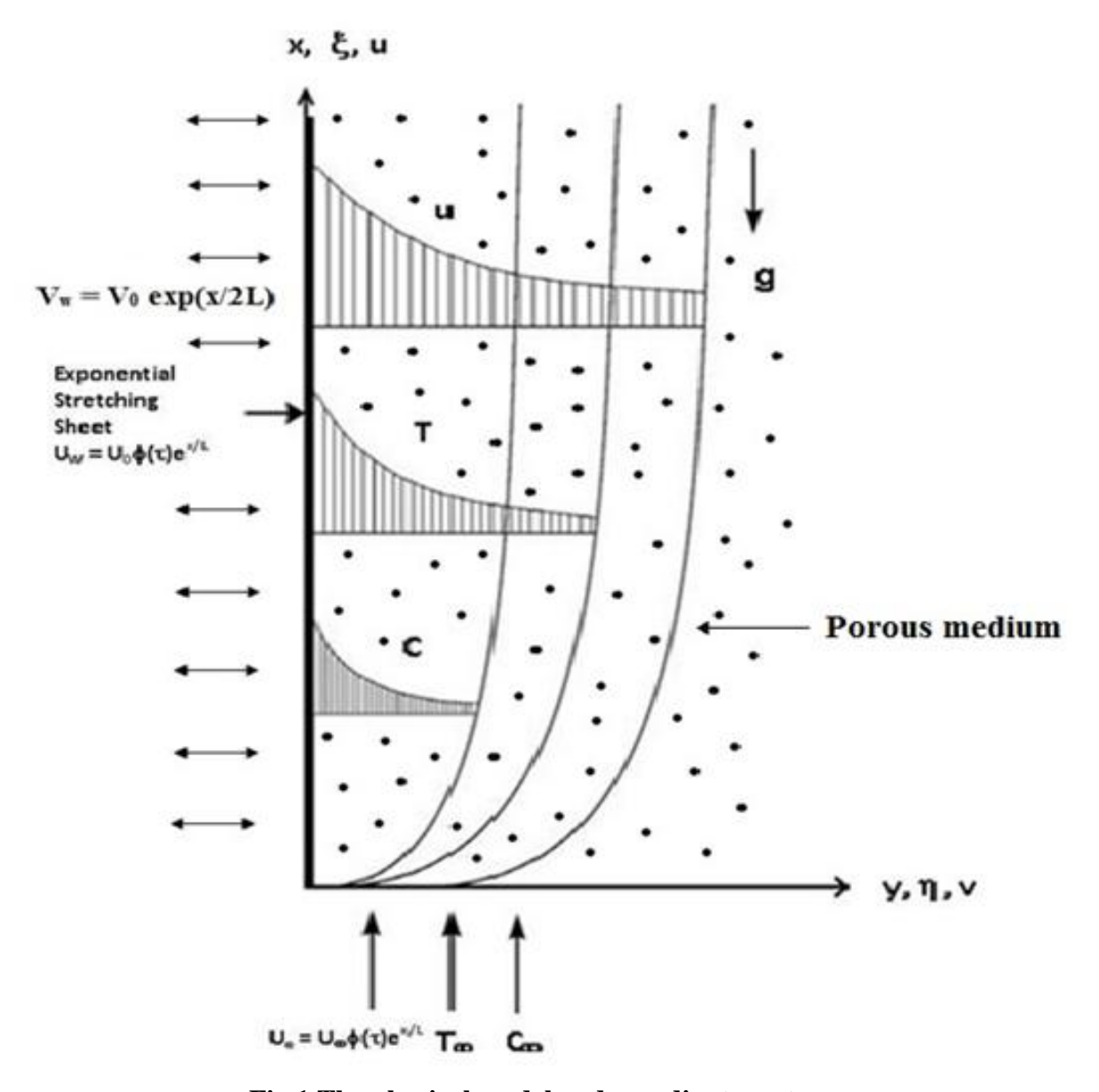


Fig.1.The physical model and coordinate system.



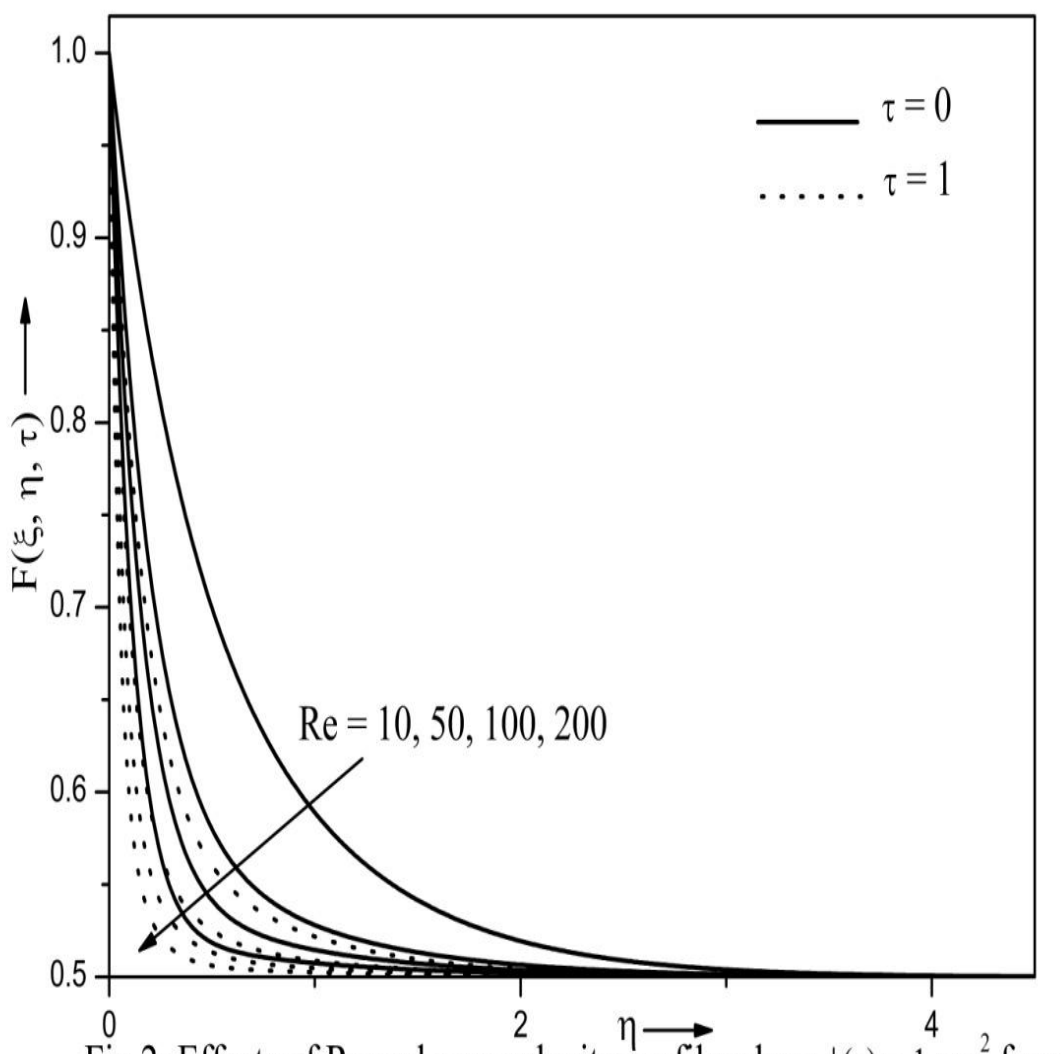


Fig 2: Effects of Re and  $\tau$  on velocity profile where  $\phi(\tau) = 1 + \alpha \tau^2$  for  $\alpha = 1.0$ , Ri = 1.0,  $\beta = 0.5$ ,  $\Gamma = 1.0$ , Pr = 0.7, Df = 0.5, Sr = 0.5, Sc = 0.94, Da = 1.0,  $\Delta = 0.5$  and A = 1.



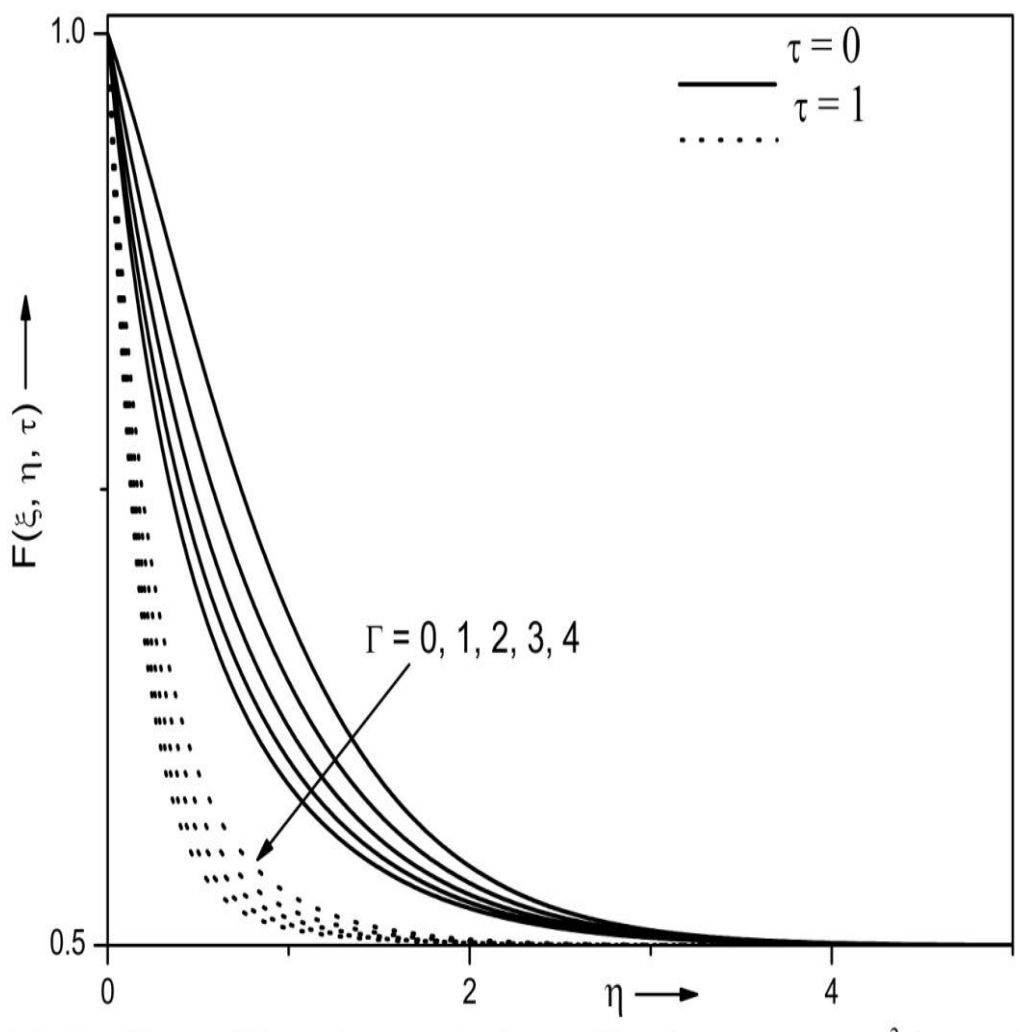
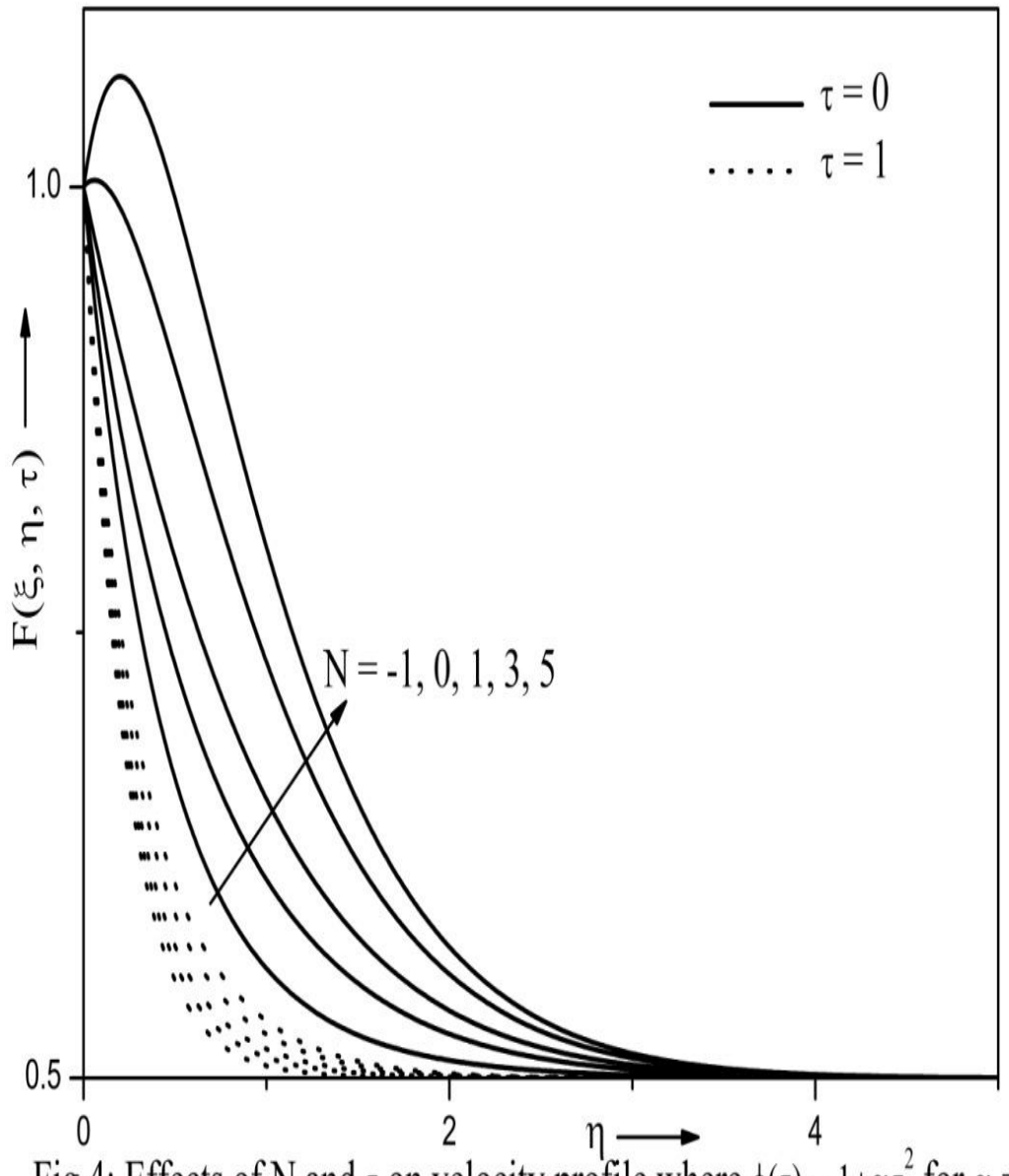


Fig 3: Effects of Re and  $\tau$  on velocity profile where  $\phi(\tau) = 1 + \alpha \tau^2$  for  $\alpha = 1.0$ , Ri = 1.0,  $\beta = 0.5$ ,  $\Gamma = 1.0$ , Pr = 0.7, Df = 0.5, Sr = 0.5, Sc = 0.94, Da = 1.0,  $\Delta = 0.5$  and A = 1.





0 2 η → 4 Fig 4: Effects of N and τ on velocity profile where  $\phi(\tau) = 1 + \alpha \tau^2$  for  $\alpha = 2.0$ , Re = 1.0, Ri = 1.0,  $\beta = 0.5$ ,  $\Gamma = 1.0$ , Pr = 0.7, Df = 0.5, Sr = 0.5, Sc = 0.94, Da = 1.0,  $\Delta = 0.5$  and A = 1.



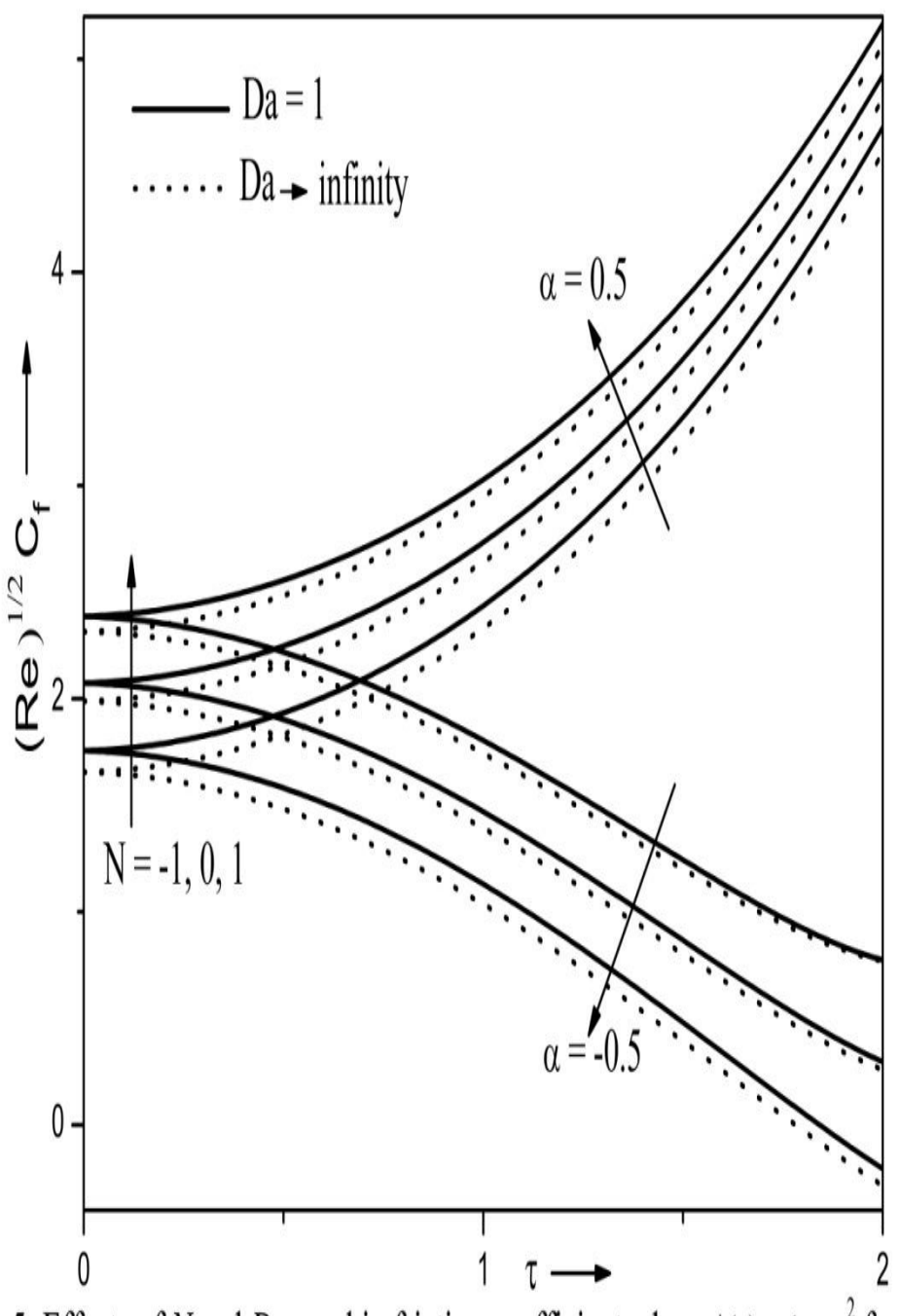


Fig 5: Effects of N and Da on skin friction coefficient where  $\phi(\tau) = 1 + \alpha \tau^2$  for  $\beta = 1.5$ ,  $\Gamma = 0.5$ , Ri = 1, Re = 2.0, Pr = 0.7, Df = 0.5, Sr = 0.5, Sc = 0.94,  $\xi = 1.0$ ,  $\Delta = 0.5$ , and A = 1.0.



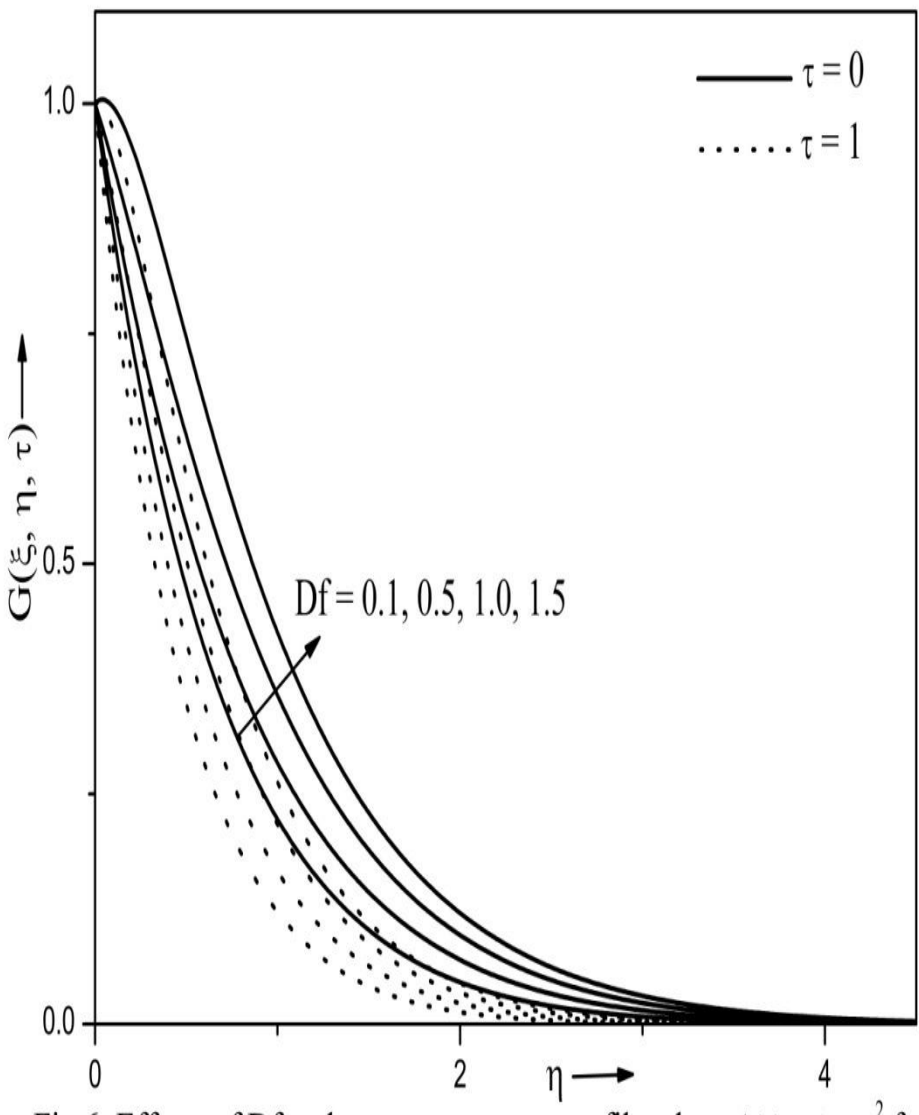


Fig 6: Effects of Df and  $\tau$  on temperature profile where  $\phi(\tau) = 1 + \alpha \tau^2$  for  $\alpha = 2.0$ , Re = 2.0, Ri = 1.0,  $\beta = 0.5$ ,  $\Gamma = 1.0$ , Pr = 0.7, N = 1.0, Sr = 0.5, Sc = 0.94, Da = 1.0,  $\Delta = 0.5$  and A = 1.



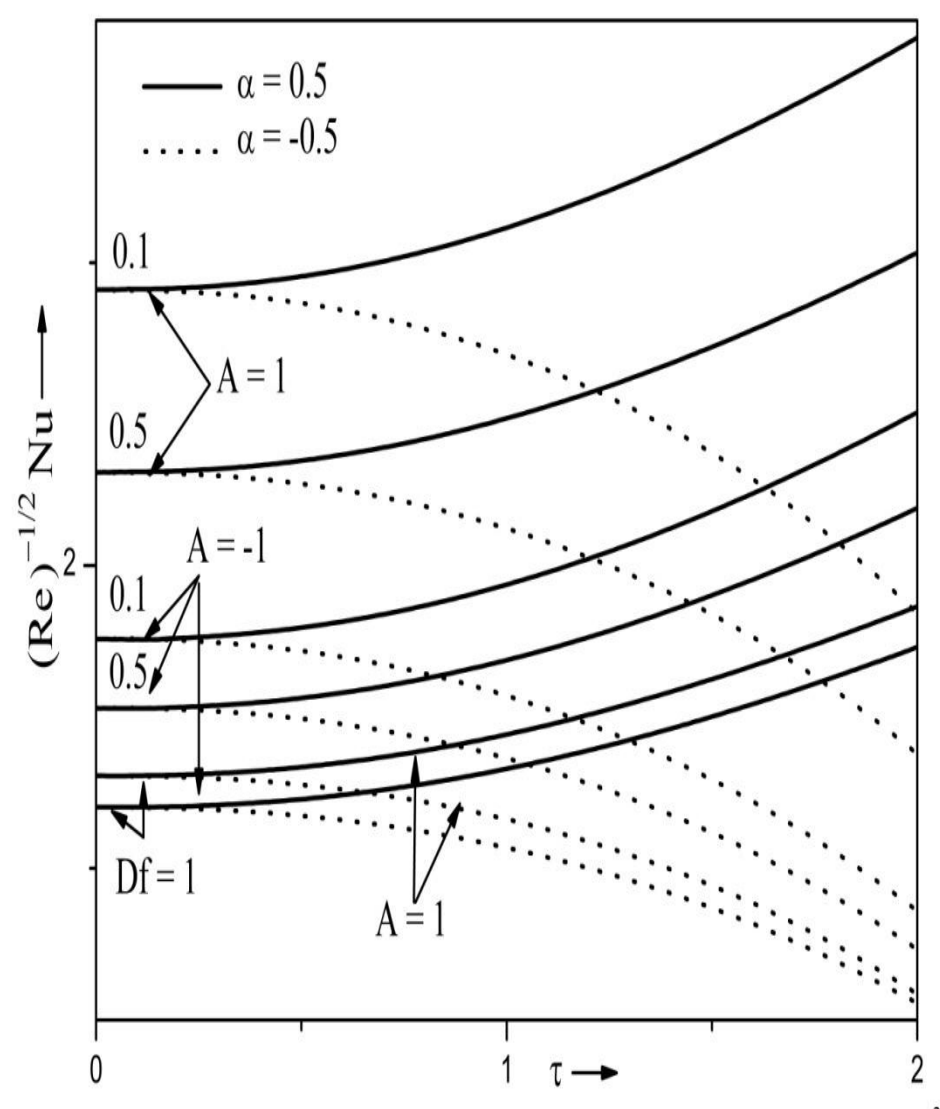


Fig 7: Effects of Df and A on heat transfer coefficient where  $\phi(\tau) = 1 + \alpha \tau^2$  for  $\beta = 1.5$ ,  $\Gamma = 0.5$ , Ri = 1, Re = 2.0, Pr = 0.7, Sr = 0.5, Sc = 0.94,  $\xi = 1.0$ ,  $\Delta = 0.5$  and Da = 1.0.



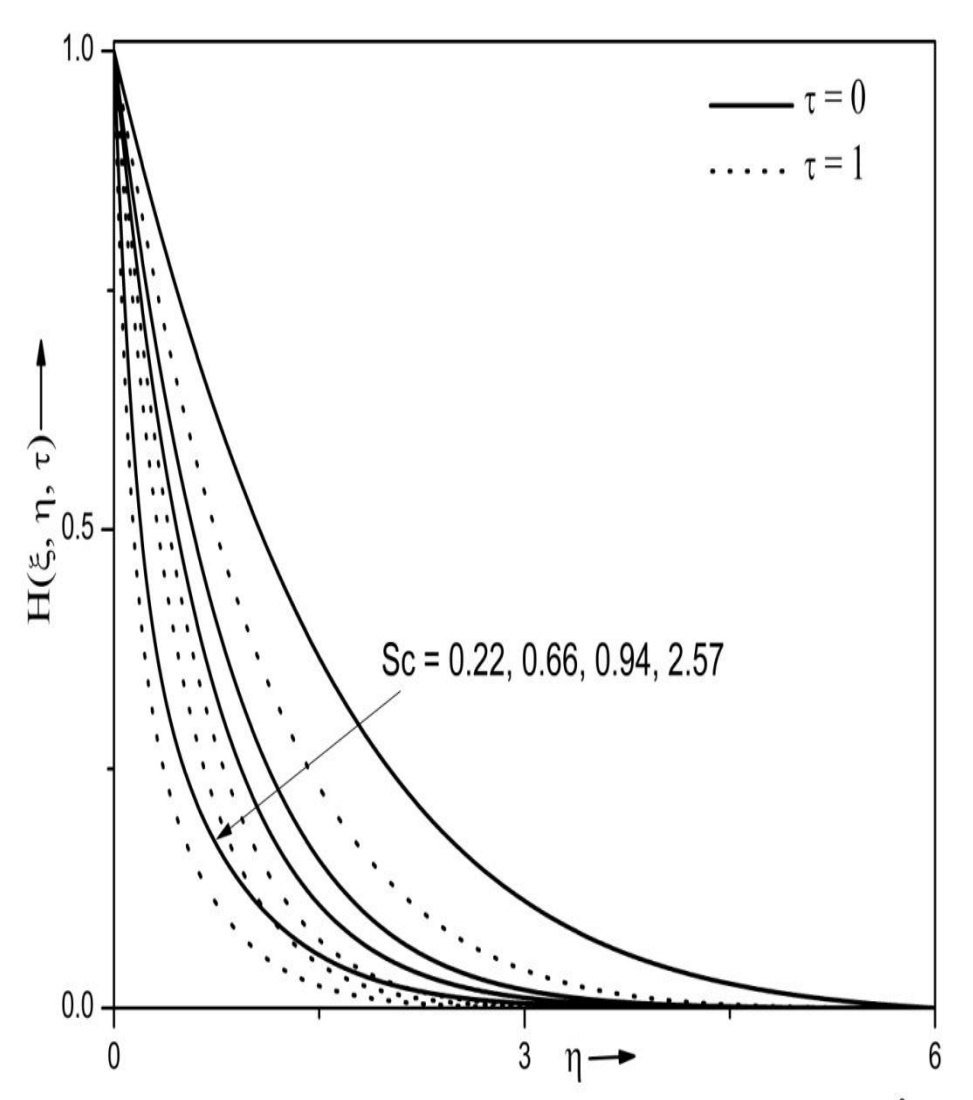


Fig 8: Effects of Sc and  $\tau$  on concentration profile where  $\phi(\tau) = 1 + \alpha \tau^2$  for  $\alpha = 1.0$ , Ri = 1.0,  $\beta = 0.5$ , N = 1.0, Pr = 0.7, Df = 0.5, Sr = 0.5, Da = 1.0,  $\Delta = -0.5$  and A = 1.



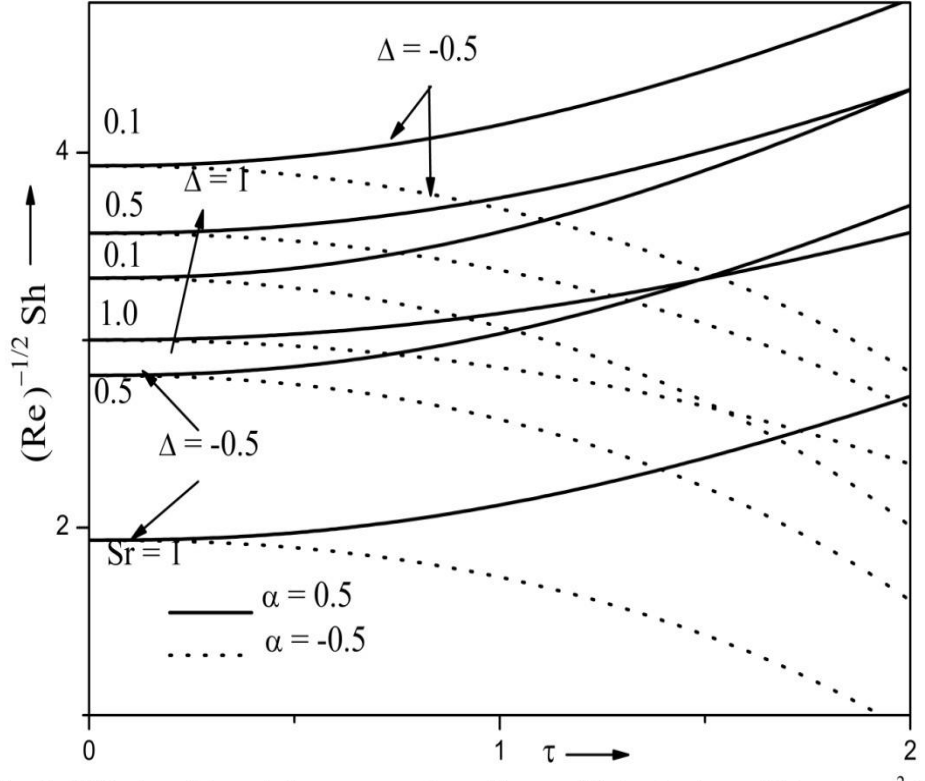


Fig 9: Effects of  $\Delta$  and Sr on mass transfer coefficient where  $\phi(\tau) = 1 + \alpha \tau^2$  for  $\beta = 1.5$ ,  $\Gamma = 0.5$ , Ri = 1, Re = 2.0, Pr = 0.7, N = 1, Sc = 0.94,  $\xi = 1.0$ , A = 1 and Da = 1.0.

